October, 2006

Semicrystalline thermoplastic elastomeric polyolefins: Advances through catalyst development and macromolecular design

Atsushi Hotta
Eric W. Cochran
Janne Ruokolainen
Vikram Khann
Glenn H. Fredrickson, et al.

Semicrystalline thermoplastic elastomeric polyolefins: Advances through catalyst development and macromolecular design

Atsushi Hotta*†, Eric Cochran*‡, Janne Ruokolainen*§, Vikram Khanna*, Glenn H. Fredrickson*¶, Edward J. Kramer*¶, Yong-Woo Shin‖, Fumihiko Shimizu‖, Anna E. Cherian, Phillip D. Hustad**††, Jeffrey M. Rose**, and Geoffrey W. Coates¶****

*Mitsubishi Chemical Center for Advanced Materials and Departments of Materials and Chemical Engineering, University of California, Santa Barbara, CA 93106; ‖Mitsubishi Chemical Group, Science and Technology Research Center, Inc., 1000 Kamoshida-cho, Aoba-ku, Yokohama 227-8502, Japan; and **Department of Chemistry and Chemical Biology, Baker Laboratory, Cornell University, Ithaca, NY 14853

Edited by Tobin J. Marks, Northwestern University, Evanston, IL, and approved July 10, 2006 (received for review April 20, 2006)

We report the design, synthesis, morphology, phase behavior, and mechanical properties of semicrystalline, polyolefin-based block copolymers. By using living, stereoselective insertion polymerization catalysts, syndiotactic polypropylene-*block*-poly(ethylene-*co*-propylene)-*block*-syndiotactic polypropylene and isotactic polypropylene-*block*-regioirregular polypropylene-*block*-isotactic polypropylene triblock copolymers were synthesized. The volume fraction and composition of the blocks, as well as the overall size of the macromolecules, were controlled by sequential synthesis of each block of the polymers. These triblock copolymers, with semicrystalline end-blocks and mid-segments with low glass-transition temperatures, show significant potential as thermoplastic elastomers. They have low Young's moduli, large strains at break, and better than 90% elastic recovery at strains of 100% or less. An isotactic polypropylene-*block*-regioirregular polypropylene-*block*-isotactic polypropylene-*block*-regioirregular polypropylene-*block*-isotactic polypropylene pentablock copolymer was synthesized that also shows exceptional elastomeric properties. Notably, microphase separation is not necessary in the semicrystalline isotactic polypropylenes to achieve good mechanical performance, unlike commercial styrenic thermoplastic elastomers.

block copolymer | polypropylene

The applications of a polymer are largely determined by its chemical, physical, and mechanical properties. These properties are in turn determined by polymer morphology, which is dictated by polymer structure and composition. Thermoplastic elastomers are a classic example where polymer architecture engenders unique properties. Block copolymers that contain at least two blocks that are hard at room temperature, separated by blocks with a glass transition temperature (T_g) below room temperature, typically exhibit elastomeric properties if the low T_g block volume is large (1–5). The most well known elastomers of this type are the polystyrene (PS)-*block* (*b*)-polybutadiene-*b*-PS triblock copolymers, sold commercially by Kraton Polymers. Such materials normally possess a microphase-separated morphology in which 10-nm-scale domains of the hard blocks (e.g., PS) are embedded as spheres or cylinders within a continuous phase of the low T_g soft blocks. The hard domains serve as thermally reversible crosslinks that at room temperature produce high levels of recoverable elasticity in the soft phase.

Sequence control of a synthetic polymer is most easily accomplished by using a synthetic technique that allows the sequential addition of one or more monomers to the macromolecule in a chain growth process without spontaneous termination. These techniques are collectively called living polymerizations, and despite many successes over the last half century, their further development remains one of the most important frontiers in polymer science. In the case of the Kraton triblock copolymers, a living anionic polymerization process is used to synthesize the materials. Because approximately two-thirds of all thermoplastic polymers are polyolefins, a significant amount of research has been directed toward the development of living catalysts for alkene polymerization. Living catalysts enabling the synthesis of block olefin copolymers have only been popularized in the last decade (6).

Block Polyolefins

There are two main ways to produce polyolefins with blocky structures: (*i*) use nonliving alkene polymerization catalysts, where changes at the site of enchainment during chain formation gives rise to different blocks in the polymer; and (*ii*) employ living catalysts, and change the monomer or reaction conditions during chain formation resulting in controlled block formation. The first approach has the advantage that more than one chain is formed per catalyst center but has the disadvantage that precise control of the number and length of blocks is not easily accomplished. Some examples of nonliving catalysts that produce olefin-based block copolymers include heterogeneous Ziegler-Natta catalysts (7), asymmetric metallocenes (8, 9), and the oscillating metallocenes (10). Although living catalysts have the inherent disadvantage that they typically only produce one chain per catalytic active center, they do have the potential for unprecedented levels of control of polymer architecture, including the composition, size, and number of blocks in olefin copolymers (6). Regarding thermoplastic elastomers, they allow the precise placement of hard blocks of high melting point (T_m) or T_g, and soft blocks of T_g well below ambient temperature. Because of the widespread use of ethylene and propylene as monomers for the synthesis of polyolefins, these monomers are prime candidates for feedstocks for thermoplastic elastomer synthesis. Isotactic or syndiotactic polypropylene (iPP or sPP) blocks, as well as linear polyethylene (PE) blocks, are obvious

Conflict of interest statement: No conflicts declared.

This article is a PNAS direct submission.

Abbreviations: *b*, *block*; iPP, isotactic PP; PEP, poly(ethylene-*co*-propylene); PP, polypropylene; PS, polystyrene; rPP, regioirregular PP; SEBS, PS-*b*-poly(ethylene-*co*-butylene)-*b*-PS; sPP, syndiotactic polypropylene; TEM, transmission electron microscopy.

†Present address: Department of Mechanical Engineering, Keio University, 3-14-1 Hiyoshi Kohoku-ku, Yokohama 223-8522, Japan.

‡Present address: Department of Chemical and Biological Engineering, Iowa State University, Ames, IA 50011.

§Present address: Department of Engineering Physics, Helsinki University of Technology, P.O. Box 2200, FIN-02015, Helsinki, Finland.

¶To whom correspondence may be addressed. E-mail: ghf@mc-cam.ucsb.edu, edkramer@mrl.ucsb.edu, or gc39@cornell.edu.

††Present address: Polyolefins and Elastomers R&D, Dow Chemical Company, 2301 North Brazosport Boulevard, B-3814, Freeport, TX 77541.

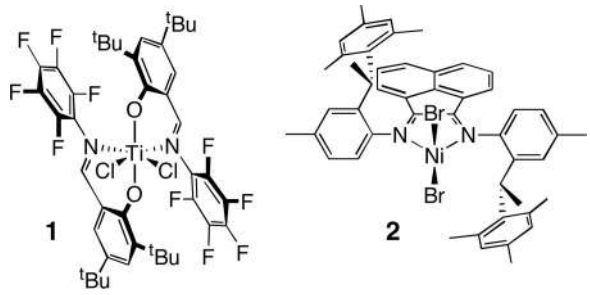

Fig. 1. Catalyst precursors for the synthesis of tactic PP block copolymers.

choices for the hard blocks, although tactic PP segments are potentially advantaged because of their higher melting temperatures and greater resistance to chain pullout from crystals. For the soft segments, random, amorphous poly(ethylene-*co*-propylene) (PEP) copolymer blocks are superior to atactic PP segments because of their significantly lower T_g values (approximately −50 versus 0°C).

Few catalysts exhibit living behavior for both the synthesis of tactic PPs and amorphous PEPs. Living, partially syndiotactic PP was first reported by Doi (11) using vanadium complexes. Coates (12) and Fujita (13) independently reported that fluorinated bis(phenoxyimine) titanium catalysts (14) are capable of the living, syndiospecific polymerization of propylene, including the synthesis of polymers with PEP blocks. Busico (15), Coates (16), and Sita (17) have reported group IV catalysts with varying degrees of isospecificity and livingness for the synthesis of iPP block copolymers. Notably, Sita (17) has recently reported the synthesis of elastomeric multiblock polymers with atactic PP and iPP segments. Coates (18) has recently reported a chiral nickel alpha-diimine catalyst that produces di- and elastomeric triblock polypropylenes with isotactic and regioirregular (rPP) PP blocks, controlled by the polymerization temperature. A possible advantage of this system is that rPP blocks are virtually indistinguishable from PEP blocks and have a suitably low T_g of approximately −55°C, enabling the synthesis of thermoplastic elastomers from a single monomer.

The focus of this article is the synthesis of thermoplastic elastomers from ethylene and propylene by using stereoselective, living alkene polymerization catalysts. Specifically, a titanium catalyst (**1**; Fig. 1) was used to synthesize a sPP-*b*-PEP-*b*-sPP triblock copolymer (***syn*TB**) by a sequential polymerization procedure (Scheme 1). A chiral nickel catalyst (**2**; Fig. 1) was used to synthesize an iPP-*b*-rPP-*b*-iPP triblock copolymer (***iso*TB**) and an iPP-*b*-rPP-*b*-iPP-*b*-rPP-*b*-iPP pentablock copolymer (***iso*PB**; Scheme 1). Herein, we show that the design and precision control of polymer structure allows for the synthesis of thermoplastic elastomeric polyolefins with unprecedented properties.

Results and Discussion

Polymer Design. Our objective in this project was to develop olefin block copolymers that could be used as thermoplastic elastomers and potentially be competitive, in cost and performance, with hydrogenated styrenic block copolymers and thermoplastic urethane elastomers. Given the limited data on olefin block copolymer systems, we attempted a design based on our experience with styrenic block copolymer elastomers. In particular, we focused primarily on triblock copolymers with two semicrystalline end blocks ("hard" blocks) and an internal amorphous, low-T_g, "soft" block. (In the case of PEP soft blocks, an ethylene mole fraction between 0.4 and 0.7 is desirable to produce a low T_g and avoid crystallization.) We also prepared and tested a pentablock copolymer with a linear hard–soft–hard–soft–hard structure. It was our expectation that good elastic recovery would require block copolymer mesophases with a continuous soft domain and discrete hard domains. Thus, we aimed for samples with 20–30% by volume of the hard blocks. In the case of styrenic elastomers, which have glassy PS hard blocks, good performance mandates that the molecular weight be adjusted so that the order–disorder transition (T_{ODT}) (2) satisfies the inequality $T_{use} < T_g < T_{ODT}$. This ensures that upon cooling from a melt processing temperature T_{proc}, block mesophases are formed before vitrification at T_g, resulting in a well ordered elastomer with glassy (and nearly pure) PS domains at the application temperature T_{use}. Ideally, for ease of processing one would like $T_{ODT} < T_{proc}$, although this is often not possible in hydrogenated PS block copolymers because of the large Flory χ parameter between PS segments and PEP or poly(ethylene-*co*-butylene) segments.

Adapting these design rules to the sPP block copolymers, we initially targeted "symmetric" sPP-*b*-PEP-*b*-sPP triblock copolymers with equal-length sPP blocks and overall molecular weight (≈350 K) consistent with the sequence $T_{use} < T_m < T_{ODT} <$

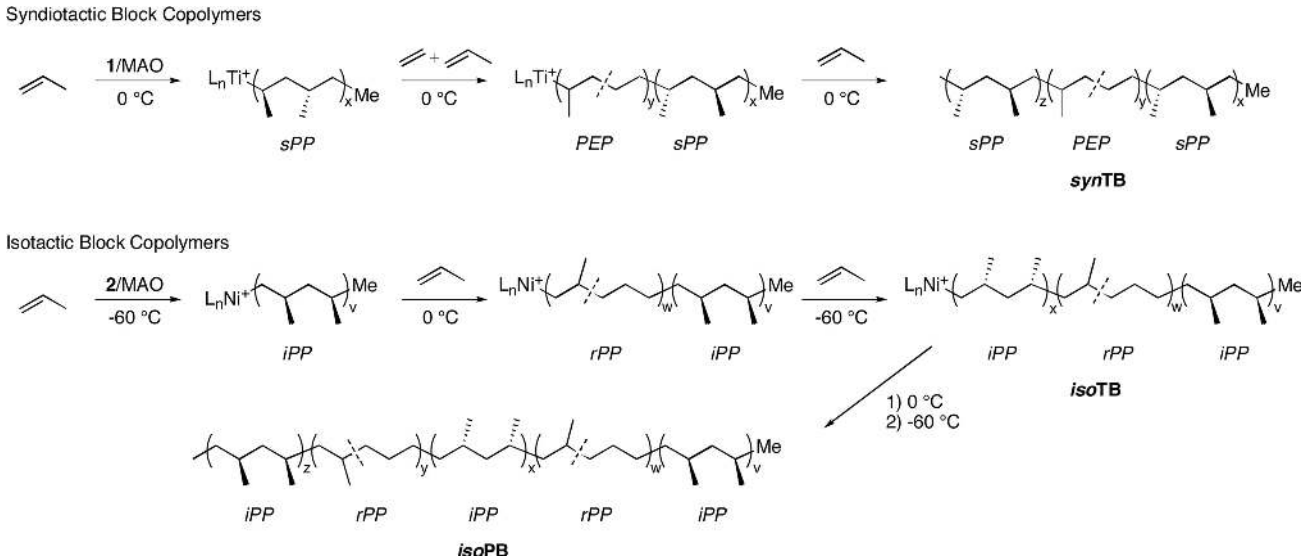

Scheme 1. Synthesis of ***syn*TB**, ***iso*TB**, and ***iso*PB**.

Table 1. Characterization of semicrystalline block copolymers

Sample	$M_{n,\,tot}$, kg/mol*	M_w/M_n	Block lengths, kg/mol	Wt. % of hard blocks†	F_e in soft blocks‡	T_m, °C§	T_g, °C§
sPP-*b*-PEP-*b*-sPP (*syn***TB**)	298	1.20*	37–225–36*	24	0.66	36, 134	−57
iPP-*b*-rPP-*b*-iPP (*iso***TB**)	109	1.14¶	10–83–16¶	24	0.53	130	−44
iPP-*b*-rPP-*b*-iPP-*b*-rPP-*b*-iPP (*iso***PB**)	159	1.39¶	16–75–6–46–16¶	24	0.53	125	−46

*Determined by using gel-permeation chromatography in 1,2-$C_6H_4Cl_2$ at 135°C versus polypropylene standards.
†Wt. % of hard blocks = $(\Sigma\, M_{n,\,hard})/(M_{n,\,tot})$.
‡Mole fraction of ethylene in PEP block (F_e) determined by ^{13}C NMR. Mole fraction of ethylene (F_e) in rPP block(s) determined by using the PP formed at 0°C by the equation: $F_e = [(1 - R)/(1 + R)]$, and $R = [CH_3]/[CH_2]$, determined by ^1H NMR.
§Determined by differential scanning calorimetry (second heat).
¶Determined by using gel-permeation chromatography in 1,2,4-$C_6H_3Cl_3$ at 140°C versus polyethylene standards.

T_{proc}. Such materials form ordered mesophases in the melt upon cooling, and the subsequent crystallization is then confined to the sPP-rich minority domains. For reasons of synthetic convenience, the iPP-*b*-rPP-*b*-iPP triblock and iPP-*b*-rPP-*b*-iPP-*b*-rPP-*b*-iPP pentablock copolymers were prepared at significantly lower overall molecular weight (≈150 K), which implies the inverted sequence (T_{use}, T_{ODT}) < T_m < T_{proc}. In these cases, crystallization occurs upon cooling from the disordered melt, so any subsequent T_{ODT} is unobservable. Because the iPP block copolymers did not possess the ideal thermal sequence based on styrenic block copolymer design, we expected that they would be inferior mechanically to the sPP block copolymers. As will be discussed below, this naïve expectation turned out to be incorrect and has highlighted an important design advantage of semicrystalline block copolymers over their amorphous counterparts.

Polymer Synthesis. Two different classes of polyolefin-based block copolymer systems were prepared. The first consists of blocks of syndiotactic polypropylene (sPP) and ethylene-propylene random copolymer (PEP). Fig. 1 shows the catalyst structure and Scheme 1 the synthetic scheme for synthesizing the block copolymers. Polymerization of propylene at 0°C resulted in a living polymerization of sPP ([*rrrr*] = 0.96). Once a block of the desired length was grown, a slight overpressure of ethylene was added and polymerized to produce a PEP block (12, 19). Triblock copolymers of sPP-*b*-PEP-*b*-sPP were synthesized by a similar procedure by adding a final polymerization of pure PP to the sequence. The sPP had a melting temperature between 130 and 146°C, decreasing with increasing molecular weight (19). For ethylene fractions (F_e) greater than 0.75 in the PEP block, crystallization of PE segments in the PEP could be detected. Synthesis of sPP-*b*-PE in which both blocks are semicrystalline was possible (19), although these were not good thermoplastic elastomers and were not considered further. The second polyolefin-based block copolymer system consists of blocks of iPP and rPP. Fig. 1 shows the catalyst structure and Scheme 1 the synthetic scheme for this block copolymer. In this case, propylene is the only monomer. When the polymerization temperature is −60°C or lower, iPP results, whereas at room temperature, the incorporation of trimethylene units [—$(CH_2)_3$—] predominates. These unbranched units are due to 3,1-insertions arising from catalyst chain-walking (18). The rPP block that results at 0°C resembles PEP (nominal F_e = 0.53) more than it does PP and in fact has a glass transition temperature (less than −40°C) that is much lower than conventional amorphous PP. As the polymerization temperature is decreased, the effective F_e decreases (0.11 at −60°C and 0 at −78°C), although the polymerization rate decreases dramatically. Triblock and pentablock copolymers can be produced simply by carrying out sequential polymerizations at different temperatures.

Polymer Morphology and Mechanical Testing. The morphology of the polyolefin block copolymers produced by these methods was determined by transmission electron microscopy (TEM) using RuO_4 to stain the amorphous regions and in selected cases by scanning force microscopy. Order–disorder transition temperatures in the melt (T_{ODT}) were determined by dynamic mechanical spectroscopy (19). Mechanical testing was performed in tension by sequentially loading and unloading, measuring the hysteresis loop and the strain not recovered after unloading.

Triblock sPP-b-PEP-b-sPP copolymers. Triblock copolymers of sPP-*b*-PEP-*b*-sPP with relatively low sPP contents (weight fractions w_{PP} < 0.3) and F_e in the PEP block <0.7 have excellent properties as thermoplastic elastomers. An example is a triblock copolymer with 25 wt % sPP, a total number average molecular weight ($M_{n,\,tot}$) of 298 kg/mol, and F_e = 0.66 (***syn*TB**; Table 1). ***syn*TB** has a microphase-separated morphology consisting of sPP cylinders in a PEP matrix as shown in the TEM micrograph in Fig. 2. The room temperature stress–strain curve for this block copolymer shown in Fig. 3 is elastomeric with an initial Young's modulus of ≈7 MPa and a strain-to-break of ≈550%. Similar results were found at an elevated testing temperature of 65°C. The elastic recovery (the fraction of the maximum applied strain recovered right after unloading) is plotted as a function of maximum strain in Fig. 4.

At maximum strains of 100% or less, the elastic recovery is better than 90%. These properties are comparable with or better than those of commercial PS-*b*-poly(ethylene-*co*-butylene)-*b*-PS (SEBS) triblock copolymers with cylindrical PS microstructures. The elastic recovery is nearly 100% in the second and subsequent cycles as long as the original maximum strain is not exceeded. As

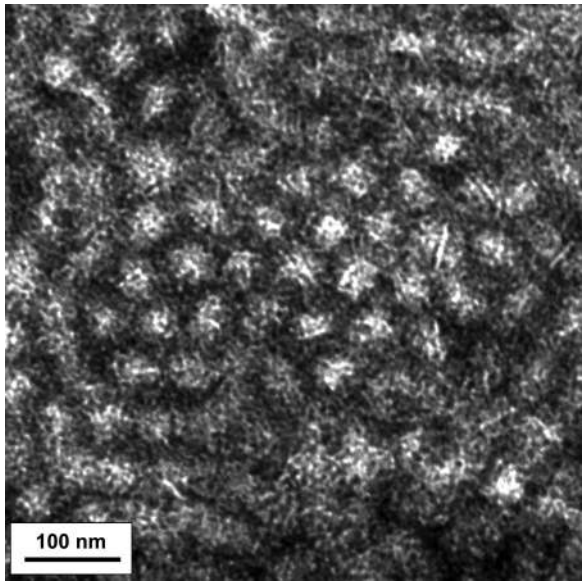

Fig. 2. TEM micrograph of ***syn*TB** (sPP cylinders are white).

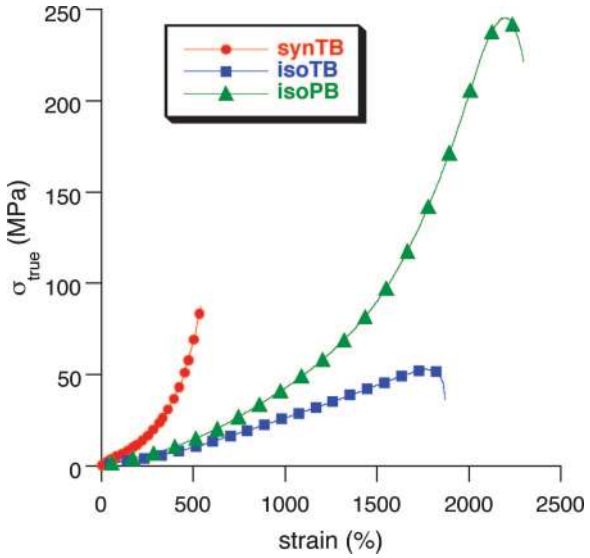

Fig. 3. Tensile true stress-versus-strain curves for ***syn*TB**, ***iso*TB**, and ***iso*PB**.

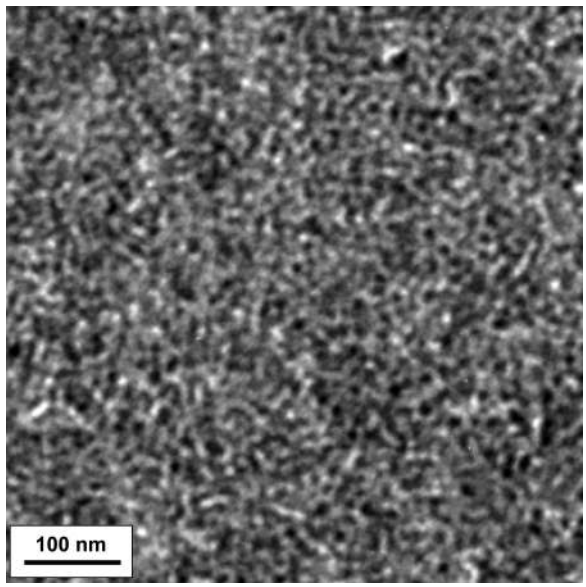

Fig. 5. TEM micrograph of ***iso*TB** showing iPP crystals but no microphase separation.

expected, triblock copolymers with larger sPP contents ($w_{PP} > 0.5$) and comparable $M_{n,\,tot}$ have microphase-separated microstructures with continuous sPP domains. While these show strains at break that exceed 500%, they also have significantly larger Young's moduli, yield behavior, and poor elastic recovery due to extensive plastic deformation of the sPP phase.

***Triblock iPP*-b-*rPP*-b-*iPP* copolymers.** Triblock iPP-*b*-rPP-*b*-iPP copolymers show even more interesting mechanical properties. As can be seen in Fig. 5, TEM analysis of an iPP-*b*-rPP-*b*-iPP block copolymer, sample ***iso*TB** (Table 1), shows no evidence of microphase separation, a finding that is consistent with its relatively low total molecular weight (109 kg/mol) and the low effective ethylene content of its rPP mid-block (19). Crystals of iPP (white) can be seen throughout the TEM image. Despite its lack of microphase separation, the elastomeric properties of the sample are exceptional. Its Young's modulus is less than half that of the sPP-*b*-PEP-*b*-sPP block copolymer, ***syn*TB**, and its strain-to-break, over 1,700%, is over three times higher (Fig. 3). In addition, it shows very good elastic recovery out to 1,000% strain as shown in Fig. 4. At a testing temperature of 65°C, the Young's modulus of sample ***iso*TB** is nearly identical to the room temperature value, as is its elastic recovery up to a strain at break of 400%.

In comparison, a microphase-separated SEBS of comparable total molecular weight (96 kg/mol) and wt % hard block (28% PS) has (at room temperature) a Young's modulus of 9 MPa, a strain to failure of 500%, and an elastic recovery of only 78% after a maximum strain of 100%. At a testing temperature of 65°C, the SEBS has a strain at break of 200% and an elastic recovery of <80%. The iPP-*b*-rPP-*b*-iPP sample, ***iso*TB**, not only has superior elastomeric properties but is much easier to process than SEBS because of the lack of microphase separation in the melt state.

Pentablock iPP*-b-*rPP*-b-*iPP*-b-*rPP*-b-*iPP* copolymers.** As a final example, an iPP-*b*-rPP-*b*-iPP-*b*-rPP-*b*-iPP pentablock copolymer was prepared with 21 wt % iPP and $M_{n,\,tot}$ = 159 kg/mol (iso*PB**; Table 1). As with its triblock counterpart ***iso*TB**, TEM analysis of ***iso*PB** shows no evidence of microphase separation, only white crystals of iPP (Fig. 6). The mechanical properties at room temperature are truly exceptional with a strain at break of 2,400% and a maximum tensile true stress of 250 MPa before break (Fig. 3). Although the elastic recovery of ***iso*PB** is lower than that of ***iso*TB** at strains of 10% and 50%, perhaps because of increasing crystal connectivity resulting from shorter rPP blocks, it rises to a value of nearly 90% out to strains of 1,000%, almost identical to ***iso*TB** (Fig. 4). The pentablock architecture (20), with an internal hard block, is apparently very effective at thwarting chain pullout from crystals at high levels of stress.

The temperature range over which these sPP and iPP block copolymers will exhibit good elastomeric properties should be limited at the low end by the glass transition temperature of the mid-block (less than −40°C) and on the upper end by the temperature at which the end blocks can be pulled free of the crystals anchoring them. The iPP blocks appear to be superior hard blocks, possibly because it is harder to remove an iPP chain from a crystal, and the middle iPP block of the pentablock also appears to thwart chain pullout. The low T_g of the soft blocks should lead to a significant improvement of low-temperature properties over atactic–isotactic stereoblock polypropylenes (10,

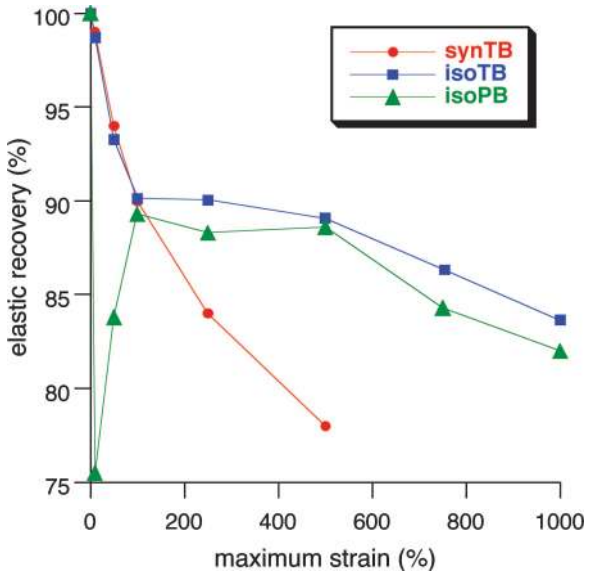

Fig. 4. Elastic recovery of ***syn*TB**, ***iso*TB**, and ***iso*PB** as a function of maximum tensile strain.

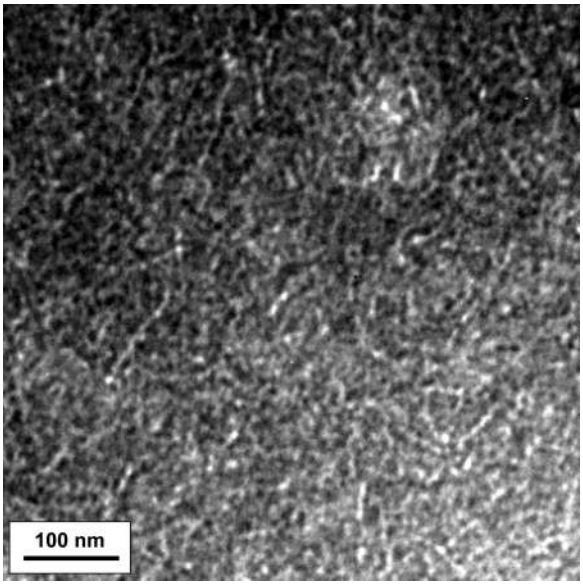

Fig. 6. TEM micrograph of ***iso*PB** showing iPP crystals but no microphase separation.

17), which have a T_g of ≈0°C. Because the melting temperature of the iPP block in ***iso*TB** is only 130°C, probably limited by occasional 3,1-insertions that introduce —$(CH_2)_3$— units into the iPP block, development of new catalysts that will improve the regioregularity of that block should lead to improvement in high-temperature strain-to-break and elastic recovery.

Conclusions

The advent of advanced catalysts for polyolefin synthesis that offer simultaneous control over molecular weight, stereochemistry, and chain termination processes has created a significant opportunity for the design of entirely new classes of polyolefin materials based on block copolymer architectures. Given the low cost and wide availability of olefinic monomers, coupled with the broad range of materials properties achievable with these new catalysts, it would seem that the area is ripe for further research, development, and commercialization.

The present work has explored only one small sector of materials design space: semicrystalline polyolefin block copolymers for use as thermoplastic elastomers. Nonetheless, we have shown the potential of polyolefin block copolymers in this sector by achieving elastomeric properties in sPP and iPP systems that rival or exceed those of commercial SEBS thermoplastic elastomers. Moreover, the polyolefin elastomers offer a considerable advantage in melt processibility, monomer cost, and potentially high-temperature performance and chemical and solvent resistance.

An important outcome of our work is that the design rules for elastomers based on semicrystalline hard blocks are more forgiving than those for traditional amorphous thermoplastic elastomers such as SEBS. The large enthalpy of crystallization overwhelms the small favorable free energy of segment mixing in low-molecular-weight block copolymers at T_m, producing a random crystal morphology with no short- or long-range order on the mesoscale. Surprisingly, this disordered morphology can possess excellent elastomeric properties that exceed those of even well microphase-separated materials. Thus, in contrast to elastomers that use glassy hard blocks, it is not necessary to maintain a high molecular weight to ensure $T_{ODT} > T_m$. This design flexibility should allow the rheological and mechanical properties of semicrystalline thermoplastic elastomers to be tuned over a much broader range.

Major challenges remaining are catalyst cost, recovery, and productivity, which are particularly acute impediments to commercialization of polymers based on living polyolefin catalysts. Now that the potential property advantages of block polyolefin materials are clear, we are optimistic that there will be a strong incentive to overcome these difficulties in both living and nonliving catalyst systems.

Materials and Methods

Polymer Synthesis. Complexes **1** and **2** were synthesized as previously reported (12, 18).

***Synthesis of sPP*-b-*PEP*-b-*sPP* (syn*TB*).** A 2-liter stainless steel autoclave was charged with PMAO (1.20 g, 20.8 mmol Al) and toluene (1 liter) under nitrogen atmosphere. The reactor was cooled to 0°C, and the atmosphere was exchanged with propylene gas and then saturated under pressure [2.0 atm (1 atm = 101.3 kPa)]. A solution of titanium complex **1** (90 mg, 0.10 mmol) in toluene (7 ml) was then added to the reactor via gas-tight syringe to initiate the polymerization. After 35 h, the unreacted propylene monomer was removed with a vacuum pump, the mixture of ethylene and propylene (32/68 mol/mol, 0.68 atm) was introduced into the reactor, and the mixture of the gas was fed to keep the pressure constant at 0.68 atm. After an additional 0.42 h, the feed of the mixed gas was stopped and the unreacted monomer gas was removed with a vacuum pump. The polymerization was allowed to continue in the presence of propylene (1.4 atm) for an additional 35 h. The reaction was then quenched by injection of methanol/HCl (25 ml, 10% vol HCl). After venting the reactor, the polymer was precipitated in copious methanol/HCl, filtered, washed with methanol, and dried *in vacuo* to constant weight (25 g).

***Synthesis of iPP*-b-*rPP*-b-*iPP* (iso*TB*).** A 6-oz Lab-Crest pressure reaction vessel equipped with a magnetic stir bar was charged with MMAO-3A (2.5 ml of a 7-wt % solution in heptane, 4 mmol Al) and toluene (30 ml) in a nitrogen-filled glovebox. The reactor was cooled to −60°C, the atmosphere was exchanged with propylene gas three times, and the flask was filled with 30 g of propylene. A solution of nickel complex **2** (17.4 mg, 0.017 mmol) in CH_2Cl_2 (2 ml) was then added to the reactor via gas-tight syringe to initiate the polymerization. After 38 h, a 2-ml sample was removed via cannula and the flask was warmed to 0°C. After stirring an additional 3.5 h, another 2-ml sample was removed, and the polymerization was cooled to −60°C and allowed to continue for an additional 76 h. The reaction was then quenched by injection of methanol/HCl (5 ml, 10% vol HCl). After venting the reactor, the polymer was precipitated in copious methanol/HCl, filtered, washed with methanol, and dried *in vacuo* to constant weight (2.45 g).

***Synthesis of iPP*-b-*rPP*-b-*iPP*-b-*rPP*-b-*iPP* (iso*PB*).** A 6-oz Lab-Crest pressure reaction vessel was prepared as described above for ***iso*TB** to generate the first iPP block. After 48 h at −60°C, a 2-ml sample was removed via cannula and the flask was warmed to 0°C. After stirring an additional 2 h, another 2-ml sample was removed and the polymerization was cooled to −60°C and allowed to continue. After 48 h, a 2-ml sample was removed via cannula and the flask was warmed to 0°C. After stirring an additional 2 h, another 2-ml sample was removed, and the polymerization was cooled to −60°C and allowed to continue for an additional 66 h. The reaction was then quenched by injection of methanol/HCl (5 ml, 10% vol HCl). After venting the reactor, the polymer was precipitated in copious methanol/HCl, filtered, washed with methanol, and dried *in vacuo* to constant weight (2.16 g).

At each stage of the polymerization, molecular weights were determined by removing an aliquot of the polymer and subjecting it to gel-permeation chromatography at elevated temperature.

Transmission Electron Microscopy. All samples for TEM were annealed in the melt for a total of 7 days, the first 4 days at 200°C to erase any previous thermal history and then an additional 3 days at a final temperature of 160°C. High-vacuum ovens [$<10^{-7}$ mbar (1 bar = 100 kPa)] were used to prevent degradation by oxidation. Melt morphology was preserved by quickly quenching the samples after annealing. TEM images of quenched samples were recorded at 200 kV with either a JEOL (Tokyo, Japan) 2000FX or an FEI (Hillsboro, OR) Technai T-20 TEM. The contrast for the morphological characterization was achieved by a sample preparation technique that relies on different rates of diffusion of a RuO_4 stain into the amorphous and semicrystalline regions (21). First, the sample surface was cut at −170°C to make a smooth surface for the stain to penetrate into the sample. The samples were then stained in a vapor of a 0.5% RuO_4 stabilized aqueous solution (Electron Microscopy Sciences, Fort Washington, PA) for a period of between 5 and 7 days. The stained sample was microtomed by using a Leica (Deerfield, IL) Ultracut UCT ultramicrotome with a diamond knife at room temperature, and 80-nm-thick sections were collected on 600-mesh hexagonal grids.

Differential Scanning Calorimetry. Polymer melting point (T_m) and glass transition temperature (T_g) were measured by differential scanning calorimetry with a TA Instruments (New Castle, DE) Q1000 calorimeter equipped with an automated sampler. Analyses were performed in crimped aluminum pans under nitrogen, and data were collected from the second heating run at a heating rate of 10°C/min from −100 to 200°C and processed with TA Instruments Q Series software.

Tensile Mechanical Testing. After the synthesis, powder materials were compression-molded into a small film ≈0.2 mm thick. Film samples were then moved into a high-vacuum oven to be annealed for 4 days (the first day at 200°C and the remaining 3 days at 160°C). After annealing, samples were cut into rectangular specimens ≈7.5 mm long, 1 mm wide, and 0.2 mm thick. Cut samples were then either stretched to fracture or up to a given tensile strain ε using an Instron (Norwood, MA) 1123 testing machine. All testing was performed at room temperature (≈20°C). The strain rate was held constant at ≈0.01/s. Two types of mechanical tests were performed as follows. (*i*) Samples were stretched monotonically to fracture, and stress–strain curves were recorded. True stresses were computed by correcting measured nominal stress values for the specimen area decrease at large tensile strains. (*ii*) Step cycle tests were performed that combine a stepwise stretching of the rectangular samples with unloading–reloading cycles. In each step, the sample was extended step by step up to strains of 10, 50, 100, 250, 500, and 750 (%). Once the sample reached the appropriate strain, the crosshead direction was reversed and the sample strain was decreased at the same rate until zero stress was achieved. The sample was then extended again at the same constant strain rate until it reached the next targeted step-strain. The step cycle test was performed until the sample fractured or until the final step of 750% was reached. With this step cycle test, we measured the elastic recovery of the materials. The elastic recovery $R(\%)$ is defined as the strain recovered upon unloading divided by the maximum strain reached during the step.

We thank the Mitsubishi Chemical Corporation for financial support of this research. This work made use of MRL Central Facilities at the University of California, Santa Barbara, which are supported by the Materials Research Science and Engineering Centers Program of the National Science Foundation under Award DMR-0520415, and of the Cornell Center for Materials Research Shared Experimental Facilities, which are supported by the Materials Research Science and Engineering Centers Program of the National Science Foundation under Award DMR-0520404. This material is based on work supported in part by the U.S. Army Research Laboratory and the U.S. Army Research Office under Grant DAAD19-02-1-0275 (Macromolecular Architecture for Performance, Multidisciplinary University Research Initiative).

1. Holden G, Kricheldorf HR, Quirk RP (2004) *Thermoplastic Elastomers* (Hanser, Munich).
2. Bates FS (1991) *Science* 251:898–905.
3. Hamley IW (1998) *The Physics of Block Copolymers* (Oxford Univ Press, Oxford).
4. Lodge TP (2003) *Macromol Chem Phys* 204:265–273.
5. Ruzette AV, Leibler L (2005) *Nat Mater* 4:19–31.
6. Coates GW, Hustad PD, Reinartz S (2002) *Angew Chem Int Ed* 41:2236–2257.
7. Collette JW, Tullock CW, MacDonald RN, Buck WH, Su ACL, Harrell JR, Mulhaupt R, Anderson BC (1989) *Macromolecules* 22:3851–3858.
8. Mallin DT, Rausch MD, Lin YG, Dong S, Chien JCW (1990) *J Am Chem Soc* 112:2030–2031.
9. Dietrich U, Hackmann M, Rieger B, Klinga M, Leskela M (1999) *J Am Chem Soc* 121:4348–4355.
10. Coates GW, Waymouth RM (1995) *Science* 267:217–219.
11. Doi Y, Keii T (1986) *Adv Polym Sci* 73/74:201–248.
12. Tian J, Hustad PD, Coates GW (2001) *J Am Chem Soc* 123:5134–5135.
13. Saito J, Mitani M, Mohri J, Ishii S, Yoshida Y, Matsugi T, Kojoh S, Kashiwa N, Fujita T (2001) *Chem Lett*, 576–577.
14. Furuyama R, Saito J, Ishii S, Makio H, Mitani M, Tanaka H, Fujita T (2005) *J Organomet Chem* 690:4398–4413.
15. Busico V, Cipullo R, Friederichs N, Ronca S, Talarico G, Togrou M, Wang B (2004) *Macromolecules* 37:8201–8203.
16. Mason AF, Coates GW (2004) *J Am Chem Soc* 126:16326–16327.
17. Harney MB, Zhang YH, Sita LR (2006) *Angew Chem Int Ed* 45:2400–2404.
18. Cherian AE, Rose JM, Lobkovsky EB, Coates GW (2005) *J Am Chem Soc* 127:13770–13771.
19. Ruokolainen J, Mezzenga R, Fredrickson GH, Kramer EJ, Hustad PD, Coates GW (2005) *Macromolecules* 38:851–860.
20. Bates FS, Fredrickson GH, Hucul D, Hahn SF (2001) *AIChE J* 47:762–765.
21. Brown GM, Butler JH (1997) *Polymer* 38:3936–3945.